

A Simple, Mechanistic Model for Directional Instability during Mitotic Chromosome Movements

Ajit P. Joglekar and Alan J. Hunt

Department of Biomedical Engineering, University of Michigan, Ann Arbor, Michigan 48109 USA

ABSTRACT During mitosis, chromosomes become attached to microtubules that emanate from the two spindle poles. Thereafter, a chromosome moves along these microtubule “tracks” as it executes a series of movements that bring it to the spindle equator. After the onset of anaphase, the sister chromatids separate and move to opposite spindle poles. These movements are often characterized by “directional instability” (a series of runs with approximately constant speed, punctuated by sudden reversals in the direction of movement). To understand mitosis, it is critical to describe the physical mechanisms that underlie the coordination of the forces that drive directional instability. We propose a simple mechanistic model that describes the origin of the forces that move chromosomes and the coordination of these forces to produce directional instability. The model demonstrates that forces, speeds, and direction of motion associated with prometaphase through anaphase chromosome movements can be predicted from the molecular kinetics of interactions between dynamic microtubules and arrays of microtubule binding sites that are linked to the chromosome by compliant elements.

INTRODUCTION

“Directional instability” is a striking feature of mitotic chromosome movements in vertebrate cells. The movements of chromosomes during prometaphase and metaphase mitosis are characterized by periods of motion at approximately constant speed, punctuated by abrupt reversals in the direction of movement (Cassimeris et al., 1994; Skibbens et al., 1993). These oscillations depend on the interactions of chromosomes with the mitotic spindle. The mitotic spindle is a fusiform structure consisting of two spindle poles from which long, thin (24-nm diameter) microtubules (MTs) radiate in all directions (e.g., Fig. 1 A). MTs polymerize from tubulin heterodimers, the asymmetry of which confers a polarity on MTs. In the mitotic spindle MTs are arrayed with their plus ends located distal to the spindle poles. The spindle serves both as scaffolding for morphological changes within a dividing cell and as a system of tracks along which chromosomes move to appropriate locations in preparation for cell division. During prometaphase mitosis, one of the two kinetochores of a chromosome binds laterally to the surface of a MT that emanates from one of the spindle poles. As the chromosome is tethered to only one pole it is said to be “monooriented.” The chromosome then becomes positioned at the end of the MT through a combination of chromosome movements and changes in the length of the MT (Rieder et al., 1990). The MT-bound kinetochore continues to accumulate MTs, and in time the unattached sister kinetochore forms connections with MTs originating from the opposing pole. The chromosome now has bipolar attachments and is said to be “bioriented” (e.g., chromosome

in Fig. 1 A). During this period directional instability commences; oscillatory movements persist throughout prometaphase and metaphase and, with decreased frequency, during anaphase. Chromosome movements are accompanied by elongation or shortening of kinetochore-associated microtubules (kMTs), primarily a result of addition or loss of tubulin subunits at the kinetochore-bound ends (Mitchison and Salmon, 1992; Wise et al., 1991; Gorbsky et al., 1987; Mitchison et al., 1986).

Both monooriented and bioriented chromosomes exhibit directional instability. After a chromosome becomes bioriented, the duration of its movements toward and away from a nearby pole are biased to bring the chromosome to the spindle equator at metaphase. Because the speed of these movements is relatively constant, the net displacement of a bioriented chromosome depends on the duration of poleward or antipoleward movements (Skibbens et al., 1993). For clarity we refer to forces and movements directed from a kinetochore toward the pole to which it is tethered as “poleward.” “Antipoleward” refers to the direction from a chromosome that is away from the nearer pole. These movements depend in part on forces generated by kMTs at the kinetochores. The forces generally stretch the two kinetochores apart, and this tension may be important for coordinating directional instability at sister kinetochores (Khodjakov and Rieder, 1996; Waters et al., 1996).

There are three established forces acting on a chromosome that can potentially bring about its poleward and antipoleward motion: 1) poleward forces that are coupled to the depolymerization of kMTs, 2) poleward forces due to minus-end directed motors that step along the surface of kMTs during early prometaphase (Rieder et al., 1990), and 3) “polar ejection” forces that push the chromosome away from a pole. In Potaroo kidney (PtK1) and Newt lung cells, polar ejection forces can push an unattached chromosome away from a nearby pole (Khodjakov et al., 1997; Ault et al., 1991; Rieder et al., 1986). Thus, these forces can po-

Submitted July 25, 2001 and accepted for publication April 18, 2002.

Address reprint requests to Ajit Joglekar, Department of Biomedical Engineering, University of Michigan, 300 N. Ingalls, Ann Arbor, MI 48109. Tel.: 734-764-3676; Fax: 734-936-2116; E-mail: ajitj@umich.edu.

© 2002 by the Biophysical Society

0006-3495/02/07/42/17 \$2.00

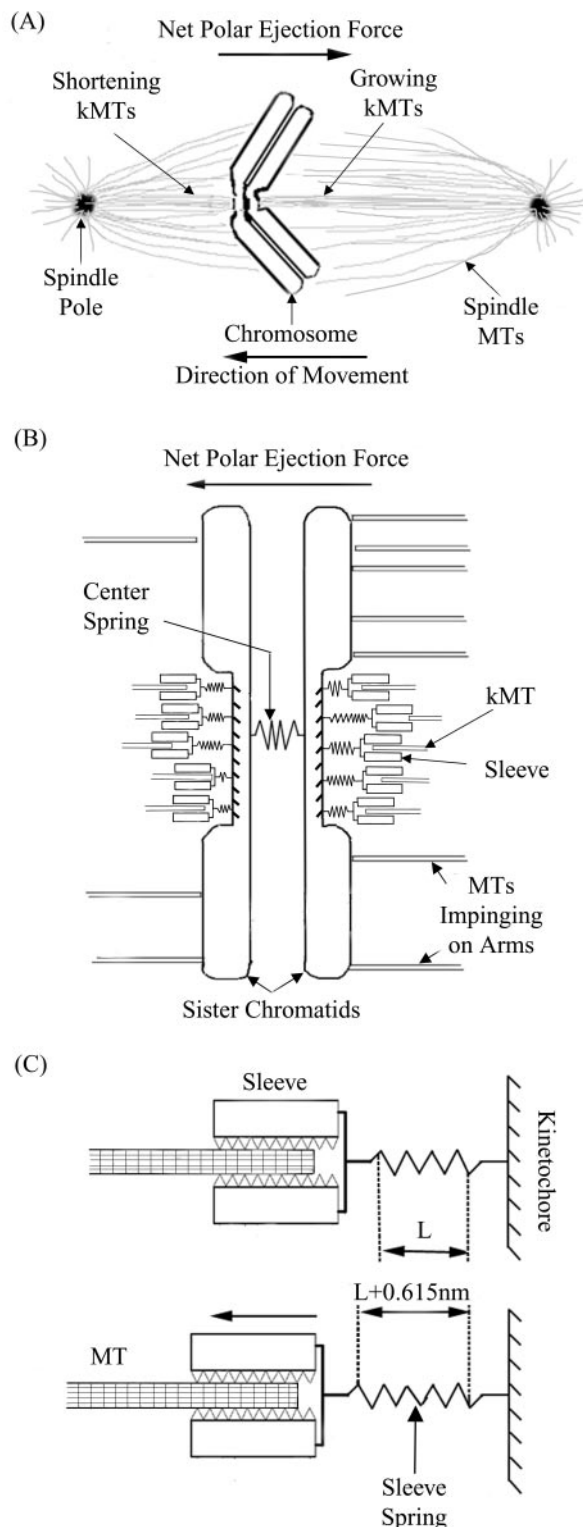


FIGURE 1 (A) Mechanics of a bioriented chromosome in the mitotic spindle. Relative scale of the chromosome has been enlarged for ease of depiction. The arms of the chromosome are swept away from the proximal pole due to polar ejection forces. (B) Mechanistic depiction of a chromosome. Each kinetochore (hash marks) has a number of MT binding sites/sleeves (number reduced for ease of depiction). The two kinetochores are connected to each other via the center spring to simulate the observed

tentially suffice for antipoleward motion of the chromosome. Polar ejection forces are likely produced by chromokinesins, motor proteins that associate with the chromosome arms, and are known to influence chromosome motion (Antonio et al., 2000; Funabiki and Murray, 2000). The ATP-dependent motor proteins dynein and centrosomal protein CENP-E have been located at the kinetochores, and changes in the activities of these proteins have complex effects on chromosome movements (McEwen et al., 2001; Yucel et al., 2000; Scharr et al., 1997; Pfarr et al., 1990). These motors may contribute to poleward chromosome movements, but the exact role has not been established. The relatively constant speed of a chromosome during poleward and antipoleward motion is difficult to explain from the behavior of conventional ATP-dependent motor proteins. The abrupt reversals in the direction of motion would require coordinated switching on and off of multiple motor molecules located at each kinetochore, separated by approximately a micrometer. The dynamics of the MTs on both kinetochores must also be coordinated: to maintain kinetochore-microtubule links, kMTs on the leading kinetochore must depolymerize, and those on the trailing kinetochore must polymerize. Whatever the mechanism that underlies this, the abrupt switching of directions must be regulated by a position sensitive mechanism so that chromosomes are correctly positioned at the onset of anaphase.

Here we present a model that can explain the directional instability of chromosomes from molecular mechanics. Integrating a wide range of experimental observations into a cohesive framework, the model can predict the forces and speeds, based on the MT dynamics associated with chromosome movements, from simple mechanics and molecular kinetics. This model generates strong, specific predictions to guide future experimentation.

MODEL

We envision directional instability to be the result of two antagonistic forces acting on a chromosome: polar ejection forces acting on the arms of the chromosome and poleward forces generated at the two kinetochores. These forces place mechanical stress on a chromosome, and their sum determines the direction of chromosome movement. The molecular kinetics of interactions between kMTs and the binding sites at the kinetochores establishes the fundamental char-

strains across the kinetochores. Each kMT interaction with a sleeve has independent rate kinetics and polymerization dynamics. The major forces acting on the chromosome are the net polar ejection force and force produced by the kMT interactions at the two kinetochores. (C) Compliance at an MT binding site on the kinetochore is represented by a sleeve spring. It gets strained by a discrete amount when the sleeve moves relative to the kinetochore. The rate kinetics of the interaction between the sleeve and kMT govern the movements of the sleeve and thus the force exerted on the kinetochore.

acter of directional instability: relatively constant speeds punctuated by sudden reversals in direction of motion. The model thus has two major aspects: the mechanics of force distribution on a chromosome, and the molecular kinetics of the interaction of kMTs with the binding sites at the kinetochores.

Mechanics

A vertebrate mitotic chromosome consists of two sister chromatids held together by a combination of DNA and protein molecules located between the kinetochores at the primary constriction. This link is represented by a linear “center spring” connecting the two chromatids (Fig. 1 *B*). The center spring simulates the observed strains between sister kinetochores, and in the context of the model it provides a mechanical coupling to coordinate the motions of the kinetochores. The stiffness of this spring (K_{Kinet}) was estimated from published observations of the strain (Cimini et al., 2001; Waters et al., 1996; Skibbens et al., 1993) and stress (Nicklas, 1988, 1983) on chromosomes. The strain data comes from mitotic chromosomes in vertebrates, whereas the stress data comes from meiotic insect cells, as this is the only system in which such measurements have been made.

Electron microscopy (EM) has revealed that the kMTs penetrate the electron-dense outer plate of the kinetochore. Based on this observation, Hill (1985) modeled interactions between a MT and the kinetochore as a “sleeve,” with a number of equidistant tubulin-dimer-binding sites on its inner surface (this is described in more detail in the next section). A kinetochore typically binds multiple MTs, and thus has multiple sleeves. From EM data (McEwen et al., 1997; McDonald et al., 1992; Rieder, 1982), we estimate the sleeve number to be ~ 35 for PtK1 cells. Because kinetochores are distorted by mitotic forces (e.g., Cimini et al., 2001), we link each “sleeve” to the kinetochores via a compliant element (Fig. 1, *B* and *C*). To estimate this stiffness (K_{sleeve}), we examined kinetochore distortions in tomographic reconstruction electron micrographs of prometaphase/metaphase PtK1 cells, which were generously provided by Dr. J. R. McIntosh and the Boulder Laboratory for 3-D Fine Structure (for detailed discussion of model parameters, see Appendix). It should be noted that a sleeve and its linking element may not be distinct entities—the compliance at the binding sites is represented by the sleeve spring.

It has been theorized that polar ejection forces, which diminish with increased distance from a pole, play a critical role in guiding chromosomes to the spindle equator during prometaphase mitosis (e.g., Rieder and Salmon, 1994). These forces sweep chromosome arms away from the spindle poles (for review, see Rieder and Salmon, 1994) and cause chromatid arms severed by microsurgery to drift away from the poles (Skibbens et al., 1995). Likewise, polar

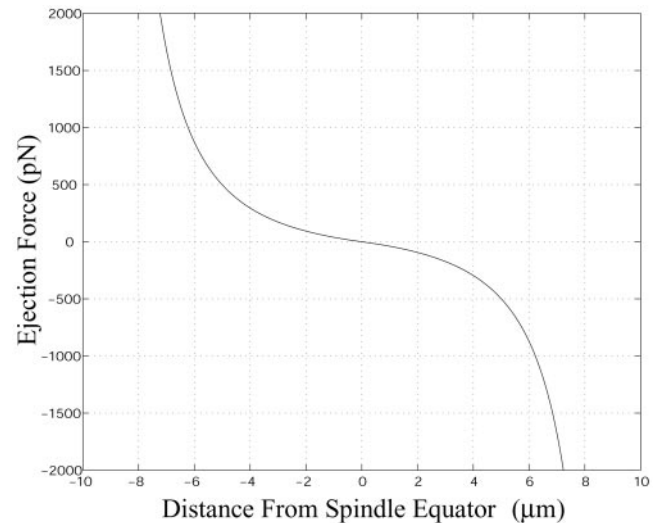


FIGURE 2 Polar ejection force distribution. Polar ejection force arises from the interaction of spindle MTs with the chromosome arms. Thus, the magnitude and direction of the ejection force is a function of the density of spindle MTs (of the same polarity) and hence the distance from the pole. We have used an inverse square relationship to model the polar ejection force as a function of distance from the spindle pole. The point where the ejection forces due to MTs from the two poles balance defines the spindle equator.

ejection forces play a crucial role in the model. We assume that polar ejection forces are developed when MTs interact with a chromosome’s arms and are directed toward the pole-distal plus ends of the MTs. Thus, the magnitude of the polar ejection force from each pole is proportional to the density of MTs emanating from that pole and the area presented normal to the spindle axis by the chromosomal arms. Consequently, the polar ejection force will be large near the pole and will drop off toward the spindle equator, where the density of MTs with opposite polarity is approximately equal. Because there are no data available on the magnitude of the polar ejection force as a function of distance from the spindle poles, we have used an inverse square distribution to provide a plausible and simple representation of this force against chromosomes of the form $\text{force} = \text{constant}/(\text{distance})^2$ (Fig. 2). Because not all MTs span the distance of a half spindle (Mastrorarde et al., 1993), the actual relationship is probably steeper than this. However, small differences in the polar ejection force distribution function have little effect on the gross behavior of the system. The polar ejection force is more important for fine-tuning directional instability, as explained in Discussion. The prefactor for the polar ejection force distribution is the only unrestricted parameter in our model.

As detailed below in Molecular Kinetics, the sleeves generate strains in the sleeve springs, which pull a kinetochore along its kMTs toward the pole. To model the net effect of this strain and the polar ejection forces, we first recognize that chromosomes move at more or less constant

speed during prometaphase-metaphase (Khodjakov and Rieder, 1996; Waters et al., 1996; Skibbens et al., 1993). Thus the forces produced at the sister kinetochores, the polar ejection forces, and viscous drag balance each other to maintain a condition of constant speed, except for brief periods when the direction abruptly reverses (Khodjakov et al., 1997; Waters et al., 1996; Skibbens et al., 1993). Because of the low Reynolds number (chromosome movements are over-damped) and the relatively small viscous load on the chromosomes (Nicklas, 1983, 1965), we can write explicit linear simultaneous equations for the force balance across a chromosome:

Left Kinetochores Force + Right Ejection Forces

$$= \text{Right Kinetochores Forces} + \text{Left Ejection Forces}$$

where, the Left and Right Kinetochores Forces are the sum of the forces contributed by the respective sleeve springs. Both sides of the equations also equal the stress in the center spring. This equation can be recast so that the positions of the left and right kinetochores are the only unknowns.

$$K_{\text{sleeve}} \sum_i (X^{\text{Left}} - S_i^{\text{Left}}) - \text{PE} = K_{\text{kinet}} (X^{\text{Right}} - X^{\text{Left}} - \gamma) \quad (1)$$

$$K_{\text{sleeve}} \sum_i (S_i^{\text{Right}} - X^{\text{Right}}) + \text{PE} = K_{\text{kinet}} (X^{\text{Right}} - X^{\text{Left}} - \gamma) \quad (2)$$

In these equations, K_{sleeve} and K_{kinet} are sleeve spring and center spring stiffness, X^{Left} and X^{Right} are the current positions of the left and right kinetochores, S_i^{Left} and S_i^{Right} are the current positions of each sleeve on the left and right kinetochores, and γ is the rest length of the center spring. The forces due to sleeve springs are summed over all the sleeves that contain kMTs. PE is the sum of the polar ejection force from both poles, the magnitude and direction of which depends upon the position of the chromosome (Fig. 2). For simplicity we have divided the ejection force equally between the two sister kinetochores. The above two equations are linear and simultaneous with two unknowns X^{Left} and X^{Right} . They are solved to obtain positions of the two kinetochores that satisfy the force balance condition. The left hand side of these equations is the total force produced at the kinetochores by strained sleeve springs and the polar ejection force, whereas the right hand side (which is the same in both equations) is the stress in the center spring.

Molecular kinetics: Hill's model

Hill's model (Hill, 1985) describes the steady-state kinetics of the interaction between a depolymerizing kMT and a binding site on a kinetochores. In this section, we discuss the fundamental properties of Hill's model. We will discuss our

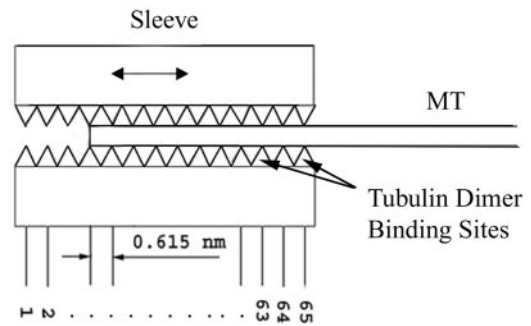


FIGURE 3 Schematic of a sleeve interacting with a MT. Tubulin binding sites are represented by triangles and are indexed from 1 (innermost) to 65. The position of the MT tip can change either by random thermal motion of the sleeve (double-headed arrow) or by addition or loss of tubulin subunits at the tip of the MT. This model provides a description of the chemical rate kinetics of the interaction between a kinetochores and a depolymerizing MT.

extension of this model to account for polymerizing MTs in the next section. Hill modeled the MT binding site on a kinetochores as a sleeve with tubulin-binding sites arranged on its inner surface (Fig. 3). The sleeve is assumed to be 40 nm long. This is equal to the thickness of the outer plate of a kinetochores, which is penetrated by a kMT (Rieder and Salmon, 1998; McEwen et al., 1993; McDonald et al., 1992). A microtubule comprises 13 protofilaments, each protofilament formed by 8-nm-long tubulin dimers lined up end-to-end. After Hill (1985), one binding site exists for each tubulin dimer located within the sleeve. Thus the smallest distance between two successive tubulin-binding sites is the minimal offset between tubulin subunits along the long axis of a MT, which is 8/13 or 0.615 nm. Thus, the total number of binding sites within a sleeve is $40/0.615 \sim 65$ (Fig. 3).

The position of the MT tip inside the sleeve, N , can change due to random thermal motion of the sleeve at a rate κ (represented by double headed arrow in Fig. 3) or due to loss of tubulin subunits at the tip of the MT. Because of interactions with the MT, the thermal motion of the sleeve occurs in discrete steps of 0.615 nm. Each additional interaction between the tubulin subunits of a MT and tubulin-binding sites on the sleeve reduces the free energy of the system by an amount "w" (Fig. 4). The sleeve, with its array of MT-binding sites, acts as a potential well that favors a deeper insertion of the MT into the sleeve to minimize the free energy of the system. An MT partially inserted into the sleeve will tend to get pulled in, so as to occupy all the binding sites (minimal free energy). Conversely, the sleeve will tend to move in the direction of the MT if the MT is anchored at its other end, for instance to the spindle poles, as assumed in this model. But repositioning of a MT within the sleeve also requires previous interactions to be broken and reformed. This poses a potential energy barrier "b" to the movement of the sleeve, and this barrier increases with

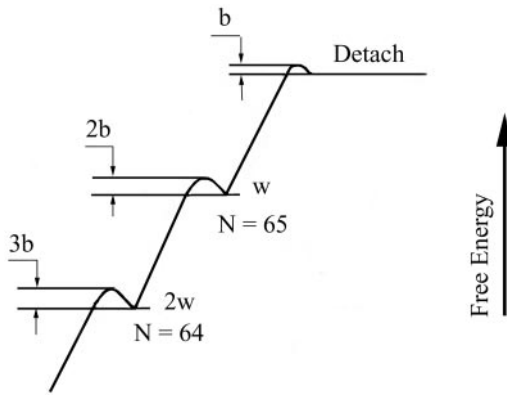


FIGURE 4 Free energy diagram for the interactions of a sleeve with a MT. $N = 65$ marks the outermost tubulin-binding site in the sleeve. Each new interaction decreases the free energy of the system by a fixed amount “ w .” The barrier to this movement due to breaking of previous bonds is indicated by “ b ” (figure adapted from Hill, 1985).

the number of interactions between a MT and MT binding sites (Fig. 4). This slows further movement of a MT into a sleeve as the MT becomes more deeply inserted. The loss of subunits shortens the MT, thus shifting the tip out of the sleeve. If the rate of tubulin loss is equal to the net rate that the MT is drawn into the sleeve, the sleeve will follow the tip of the depolymerizing MT with constant average speed.

Using detailed balance arguments, the steady-state transition rates can be written as shown in Eq. 3.

$$N - 1 \xrightleftharpoons[\kappa \times r^{M-N} \times f]{\kappa \times s \times r^{M-N} \times f^{-1} + \beta \times s} N \quad (3)$$

The parameters in this equation are as follows.

N and $N - 1$ are positions of MT tip inside the sleeve (see Fig. 3). The $N - 1$ to N transition rate (k_{out}) describes tip movement out of the sleeve. The reverse rate is k_{in} .

κ is the constant that describes the rate of thermal movements of the sleeve over the distance between tubulin binding sites in the absence of potential energy barriers due to interactions with a bound MT (Fig. 3). The step length for this movement is 0.615 nm.

When an MT moves into the sleeve (N to $N - 1$) it binds an additional tubulin-binding site, and the total free energy decreases. Conversely, movement of the MT out of the sleeve increases the free energy of the system by an amount “ w .” The net effect is to decrease k_{out} relative to k_{in} . The prefactor, $s = e^{w/kT}$, takes this into account. It also reduces the rate of loss of tubulin subunits from the MT tip inside a sleeve ($\beta \times s$). The value of s was chosen to account for the decreased rate of shortening of kMTs. This implies that when tubulin subunits leave the tip of a MT, their dissociation from binding sites in the sleeve is assisted by energy released from the MT lattice. For a more thorough discussion see Hill (1985).

Relative movement between the MT and the sleeve implies breaking and reforming bonds with the sleeve, thus there is a potential barrier to such movements. This barrier, $r = e^{-b/kT}$, increases as the power of number of interactions ($M - N$), in which M is the total number of binding sites in a sleeve plus one ($M = 66$) and N is the current position of the MT tip inside the sleeve.

$f (= e^{-F \times l / 2kT})$ is the Boltzman factor representing the effect of load on the rate kinetics. The numerator of the exponent is the mechanical work done in pulling the sleeve through a distance l (0.615 nm) against a tension F . In the denominator, which accounts for thermal energy, k is the Boltzman constant, and T is absolute temperature. In the absence of a better estimate, the effect of load is assumed to affect both forward and backward rate equally (hence the factor of 2 in the denominator). Tension ($f < 1$) tends to pull a MT out of the sleeve, whereas compression ($f > 1$) assists further advance into the sleeve.

β is the rate at which tubulin subunits are lost from the tip of a depolymerizing MT.

A more complete description of these parameters and their calculation can be found in Hill (1987, 1985). Both rates are a function of MT tip position and the load on the MT. k_{out} is the sum of two effects: 1) the probability of MT tip position inside a sleeve changing due to thermal motion of the sleeve and 2) the probability of the tip changing position through loss of tubulin subunits. Fig. 5, A and B show the effect of tension on the steady-state probability distribution for the MT tip position inside a sleeve. The maximal probability position shifts outward with increased tension (Fig. 5 A). This occurs because tension increases k_{out} and decreases k_{in} . These rates are rebalanced when the tip shifts to a position where the factor r^{M-N} restores these rates to equilibrium. Fig. 5 B is a plot of maximum probability position as a function of tension. The maximum probability position is the same as the steady-state position, and can be solved analytically by setting k_{out} equal to k_{in} (Eq. 4).

$$N_{\text{max}} = M + (\ln r)^{-1} \ln \left[\frac{\kappa f (1 - s f^{-2})}{\beta s - \alpha} \right] \quad (4)$$

An important characteristic of Hill’s model is that over a wide range of increasing tension, the speed of depolymerization-coupled movements will remain constant. This behavior arises because at steady state, by definition, the average position of the kMT tip within the sleeve is invariant, and thus the sleeve moves at an average speed equal to the rate of kMT shortening. That is, the sleeve keeps up with the tip of the depolymerizing MT. If the tension on a sleeve changes, the sleeve will shift to a new maximal probability position (Fig. 5 A), where it will continue on at the rate of kMT shortening. Put another way, the force generated by a sleeve adapts to an opposing load to maintain constant speed. This is an important distinction from conventional

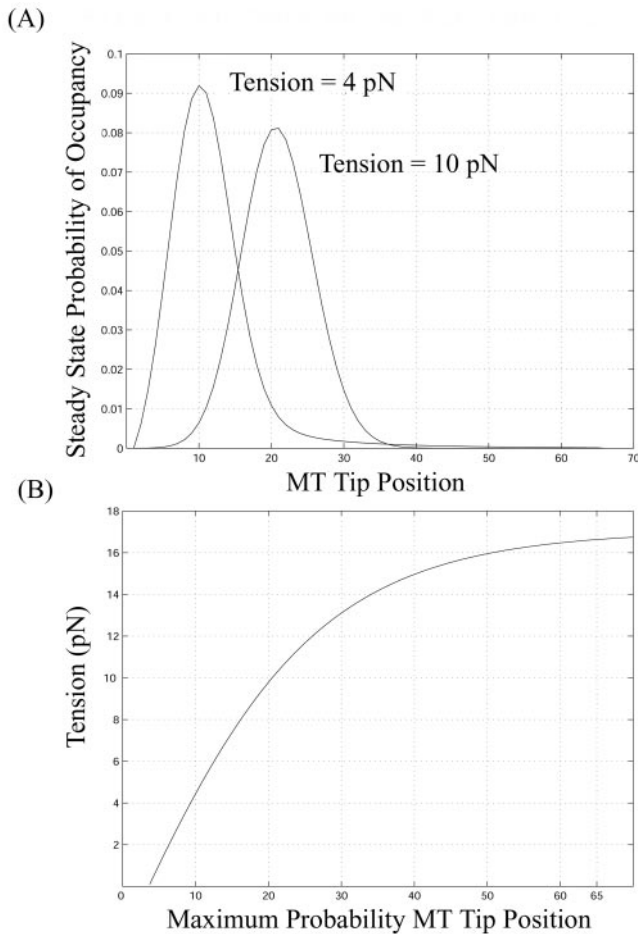


FIGURE 5 (A) Effect of tension on a sleeve-MT interaction. The steady-state probability distribution of a depolymerizing MT tip inside the sleeve is given by Hill's equations. As tension on the MT increases, the maximum probability position of the MT tip shifts outwards in the sleeve. (B) Maximum probability tip position plotted as a function of tension according to Eq. 4.

ATP-dependent motor proteins, in which the speed decreases monotonically as the load is increased (Schnitzer et al., 2000; Meyhofer and Howard, 1995; Svoboda and Block, 1994; Hunt et al., 1994; Oiwa and Takahashi, 1988; Hill, 1938). Of course no motor can adapt to an infinite range of loads: if sufficiently loaded a motor will fail. In the case of the sleeves, failure occurs when there is a significant probability of the kMT tip leaving the sleeve altogether (i.e., $N > 65$).

To reiterate, the defining features of the sleeve motors are: 1) over a wide range of increasing loads the speed of depolymerization-coupled movement of a sleeve is unaffected, and 2) the probability of kMT dissociation from a sleeve increases with the load. It is noteworthy that the basic behaviors of this model are not highly sensitive to the specific values of the parameters used. The values of these parameters are given in Table 1. Hill's treatment provides the general framework for modeling the interaction between

a MT and a sleeve, which we extend to account for the full range of microtubule polymerization dynamics.

Molecular kinetics: polymerizing MTs

In vitro MTs spontaneously alternate between periods of slow polymerization (growth) and fast depolymerization (rapid shortening). Transitions from growth to rapid shortening are called "catastrophes." This process is known as "dynamic instability" (Mitchison and Kirschner, 1984; for review, see Desai and Mitchison, 1997), and it is driven by the energy of hydrolysis of tubulin-bound guanosine triphosphate (GTP). MTs in the mitotic spindle also alternate between periods of shortening and elongation at their ends distal to the spindle poles. Structural and biochemical data suggest that a large portion of the energy released during GTP hydrolysis is stored in the microtubule lattice (Mickey and Howard, 1995; Caplow et al., 1994). Implicit in Hill's model is that this energy supports the movements of a kinetochore-bound sleeve.

Hill's model considers only depolymerizing MTs. We extend the rate equations to account for polymerizing MTs (Eq. 5). During rapid shortening, the free ends of MTs depolymerize faster than chromosomes move (Rusan et al., 2001; Skibbens et al., 1993; Walker et al., 1988). Therefore, only growing MTs can enter empty sleeves at a rate k_{on} (see Appendix). After entering a sleeve, the kMTs then switch to the shortening state at a rate k_{cat} (see Appendix). A polymerizing MT can advance relative to the sleeve by the addition of subunits at its tip. To account for this a factor " α " equal to the rate of subunit addition at the plus end of a kMT, is added to k_{in} .

$$N - 1 \xrightleftharpoons[\kappa \times r^{M-N} \times f + \alpha]{\kappa \times s \times r^{M-N} \times f^{-1}} N \quad (5)$$

The in vivo polymerization rate of nonkinetochore MTs in mitotic pig kidney LLCPK-1 cells has been measured to be ~ 350 subunits/s ($13 \mu\text{m}/\text{min}$) (Rusan et al., 2001). We assume that the dense structure of a kinetochore sterically shields kMTs from the factors that increase the polymerization rate in the cytoplasm and use 40 subunits/s, a typical polymerization rate for isolated microtubules at physiological temperature (Walker et al., 1988). This supposition, although plausible, is without direct experimental justification. It is necessary to prevent chromosomes from moving at nonphysiological speeds when subject to large polar ejection forces. This is discussed further in Results.

The possibility of a polymerizing MT growing beyond the sleeve requires additional consideration. When an MT penetrates the sleeve completely, there is no longer a potential change associated with movement of the sleeve relative to the MT (e.g., tip shifting from $N = 1$ to 0), because all binding sites are now occupied. As a result, the modi-

TABLE 1 Table of Parameters*

Parameter	Description	Value	Unit
κ	Rate constant for discrete steps of 0.615 nm of the chromosome	1800 (7200) [†]	s ⁻¹
s	Factor to account for the slowing of transition rates due to the free energy increase associated with the loss of an interaction between a tubulin subunit and a binding site in the sleeve	33/340	
r	Factor to account for the potential barrier to the movement of a MT in a sleeve due to breaking and reforming existing interactions	0.96	
f	Factor to account for the effect of load on the chemical kinetics of the system	≥ 0	
β	Rate of losing subunits from a free MT tip [‡]	340	s ⁻¹
α	Rate of adding subunits at a free MT tip [§]	350	s ⁻¹
M	Total number of binding sites inside a sleeve plus one	66	
N	Current position of MT tip inside the sleeve	(1–65)	
	Number of sleeves on a kinetochore	35	
k_{cat}	Rate of catastrophe for a MT	2.5×10^{-3}	s ⁻¹
k_{on}	Rate of capturing a growing MT	6.2×10^{-3}	s ⁻¹
γ	Rest length of the center spring	0.5	μm
K_{kinet}	Stiffness of the center spring	0.1	pN/nm
K_{sleeve}	Stiffness of a sleeve spring	0.07	pN/nm

*An explanation for the choice of values for new parameters can be found in the *Appendix*.

[†]See *Appendix*.

[‡]Walker et al., 1988.

[§]Rusan et al., 2001.

fying factor, s , drops out of the backward rate k_{out} ($s = 1$). The sleeve now slides on the MT with its motion being resisted only by the potential energy barrier associated with breaking interactions between tubulin subunits and their binding sites. The direction of this movement is unbiased in the absence of tension on the system ($f = 1$). Likewise, if thermal movements bring the tip of a shortening MT beyond the sleeve, the MT reverts to subunit loss at the depolymerization rate of a “free” MT (340 subunits/s). Eqs. 6 and 7 describe the transition rates for MTs that occupy all the tubulin-binding sites in the sleeve ($N < 1$).

$$0 \xrightleftharpoons[\kappa \times r^M \times f]{\kappa \times r^M \times f^{-1} + \beta} 1 \quad (6)$$

$$0 \xrightleftharpoons[\kappa \times r^M \times f + \alpha]{\kappa \times r^M \times f^{-1}} 1 \quad (7)$$

Eq. 6 applies to depolymerizing kMTs and Eq. 7 to polymerizing. We allow an MT to penetrate and extend beyond the sleeve a small number of subunits (five), before it encounters a barrier corresponding to the inner plate of the kinetochore, through which MTs do not penetrate (McDonald et al., 1992; Rieder, 1982). When the MT encounters this boundary, it is not allowed to acquire any more subunits. The MT can then gain subunits only if the entire sleeve moves toward the chromosome, making room for an incoming subunit, and will lose a subunit if the sleeve moves toward the MT. This implies that an MT at the boundary has stalled; in the absence of an external force the probabilities of subunit gain or loss are equal.

A more rigorous treatment of a MT growing against a barrier suggests the rate of subunit addition drops monotonically as the resisting force on the tip increases (Kolomeisky and Fisher, 2001; Doorn et al., 2000; Mogilner and Oster, 1999; Hill, 1987, 1985). When the resisting force equals the stall force, the rates of subunit loss and addition come into equilibrium. We have approximated this for the case in which the stall force is very small relative to other forces on a chromosome. In vitro, polymerizing MTs growing against a barrier can generate a force of ~ 4 pN (Dogterom and Yurke, 1997). But data obtained from oscillating mitotic newt lung and PtK1 cells suggests that kinetochores are, on average, under tension and rarely push (Khodjakov and Rieder, 1996; Waters et al., 1996), and the force generated at the kinetochore during MT polymerization in vitro is less than 2 pN (Hunt and McIntosh, 1998). Hence, we have assumed that for practical purposes polymerizing kMTs do not exert any force on the kinetochore. If polymerizing kMTs exert a force that is less than ~ 1.0 pN, the fundamental behavior of the system does not change. For larger forces, such as 4 pN, the model predicts that chromosome movements should frequently stall and that the kinetochores should be compressed together for extended periods. Both of these behaviors are inconsistent with the observed behavior of mitotic chromosomes. We are currently pursuing experiments to determine the forces generated by MT polymerization at the kinetochore.

SIMULATION

The simulation was stochastically modeled using MATLAB (The Mathworks, Inc., Natick, MA) by an iterative process.

In each iteration, the forward and backward rate constants are calculated for each kMT inside a sleeve. The rates, k_{in} and k_{out} are then compared with a randomly generated number, $0 < n < 1$, to determine if a microtubule tip moves in ($n < (k_{in} \times \text{time between iterations})$) or out ($n > (1 - (k_{out} \times \text{time between iterations}))$), or stays at the same position in the sleeve. To minimize the likelihood of events being missed (e.g., two steps in rapid succession), iterations correspond to 0.001-s intervals, which is short relative to typical values of k_{in}^{-1} and k_{out}^{-1} . A change in the position of the kMT tip within a sleeve indicates that either the MT added/lost subunits, or the sleeve moved toward/away from the MT (due to its thermal motion). Tip movements due to the later processes stretch or relax the sleeve spring, depending upon the direction of the sleeve movement. As explained earlier (Mechanics), the net forces on both kinetochores together with the polar ejection force must balance. The positions of the two kinetochores are adjusted so as to achieve this condition according to Eqs. 1 and 2. These equations are solved to obtain the new positions of the two kinetochores, which satisfy the force balance condition. Once the current positions of the kinetochores are known, the strain in each of the sleeve springs can be recalculated. Thus, the force on each of the individual sleeve springs becomes known. This is then used to calculate the factor, f , used in computing the dynamics of the kMT/sleeve interactions for the next iteration. Any kMT that moves to a position $N > 65$ detaches, leaving an empty sleeve. The occurrence of a growing MT entering a sleeve and a growing kMT switching to rapid shortening are calculated from k_{on} and k_{cat} respectively, in the same manner that k_{in} and k_{out} are applied to predict the movement of a kMT tip within the sleeve.

Table 1 gives a list of parameters used in our model. The reasoning behind the estimation of these parameters is outlined in the Appendix.

RESULTS

Fig. 6 shows a simulation of bioriented chromosome movements during prometaphase/metaphase. The chromosome was initially positioned at the spindle equator ($10 \mu\text{m}$) with the maximal number (35) of kMTs on both kinetochores. The left kinetochore has five depolymerizing kMTs to start with; the right kinetochore has only polymerizing kMTs. As a result, the left kinetochore leads the initial run of the chromosome toward the left pole. The excursions of the chromosome during the larger oscillations are ~ 1 to $1.5 \mu\text{m}$ in either direction, comparable with the observations in PtK1 cells (Khodjakov et al., 1997; Khodjakov and Rieder, 1996). Fig. 6, B and C show the number of pre and post-catastrophe kMTs on each kinetochore. Note that post-catastrophe microtubules accumulate at the leading kinetochore, but are lost when the chromosome switches directions. The average speed of chromosome movement was $\sim 17 \text{ nm/s}$

($\sim 1 \mu\text{m}/\text{min}$) in either direction. The stress in the center spring, which is directly proportional to the separation of the two kinetochores, attained values as high as 60 pN (Fig. 6 D). The chromosome typically switched directions when the stress in the central spring was between 30 and 60 pN; this value varies due to the stochastic nature of the model. The ejection force reached a maximal value of $\sim 100 \text{ pN}$. In PtK1 cells it has been observed that bioriented chromosomes sometimes switch from directed motion to relatively stationary state for extended periods of time (Khodjakov et al., 1997; Khodjakov and Rieder, 1996). This is apparent in our simulation (Fig. 6 A). According to our model, consistent poleward motion of the chromosome depends on one of the kinetochores accumulating a sufficient number of depolymerizing MTs. This critically depends on kMT dynamics, and we find the turnover of kMTs in PtK1 cells (Zhai et al., 1995) is such that chromosomes exist at the border between exhibiting consistent oscillations and less directed movement. With a small increase in the turnover rate, oscillations will become more regular like those observed in Newt lung cells (Waters et al., 1996; Skibbens et al., 1993), although we note that Newt chromosomes also exhibit periods of less directed motion. Based on the measurements of the density of MTs of the same polarity at the spindle equator ($\sim 15 \text{ MTs}/\mu\text{m}^2$), at metaphase in PtK cells (Mastrorarde et al., 1993), and assuming chromosome cross-sectional area of $\sim 14 \mu\text{m}^2$ normal to the plane of the spindle, the value of the prefactor used for the inverse square polar ejection force distribution (ejection force of 100 pN, $2 \mu\text{m}$ away from the spindle equator) implies a force of $\sim 0.3 \text{ pN}$ per spindle MT interacting with the chromosome arms.

The model can also simulate the motions of a monooriented chromosome (Fig. 7). The chromosome initially has three depolymerizing and seven polymerizing kMTs on the left kinetochore facing the pole, which is $\sim 5 \mu\text{m}$ away. To simulate transition to biorientation, the right kinetochore is allowed to begin accumulating MTs after the first 1500 s of the simulation (Fig. 7 C); some switch to depolymerization and then drag the chromosome toward the spindle equator. This simulates the congression of the now bioriented chromosome to the spindle equator. The monopolar chromosome undergoes regular oscillations with the poleward movement of the chromosome in phase with the accumulation of depolymerizing kMTs at the attached kinetochore (Fig. 7, A and B). The corresponding strain in the center spring varies from 0 to 50 pN (Fig. 7 D). The peak-to-peak amplitude of the oscillations is $\sim 1.5 \mu\text{m}$, which is approximately the same as published observations of monooriented chromosomes during early prometaphase (Khodjakov and Rieder, 1996). The ejection force distribution for the monopolar chromosome also follows an inverse square law, however prefactor was reduced so that the oscillations are appropriately near the pole. This is reasonable because, at the start of prometaphase, the arrays of MTs at spindle poles

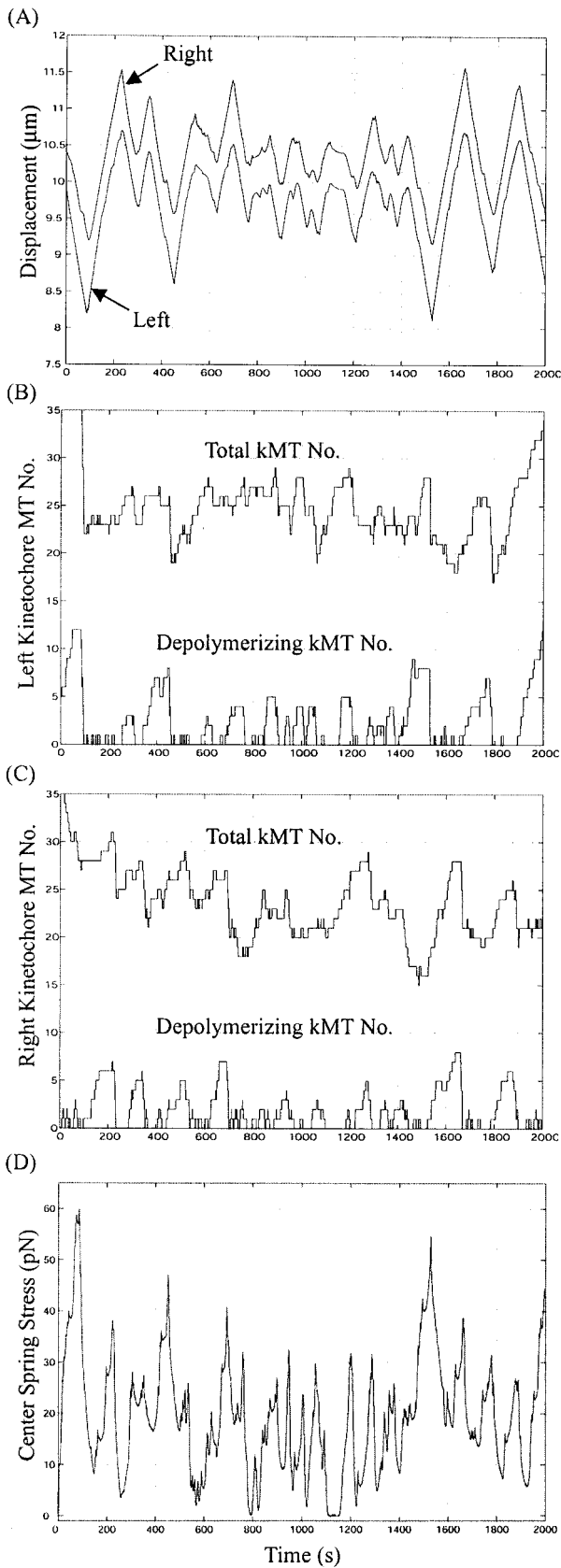


FIGURE 6 (A) Simulated motion of a bioriented chromosome. Spindle equator is located at $10 \mu\text{m}$. Both kinetochores start out with 35 kMTs at

are not fully developed. The polar ejection force presumably evolve with the MT arrays from both the poles.

As pointed out earlier, we use the in vitro polymerization rate for kMTs inside the sleeve, rather than the faster rate observed at the end of nonkinetochore MTs in vivo. If we instead raise the kMT polymerization rate to that at the ends of nonkinetochore MTs in mitotic cells (Rusan et al., 2001) we observe a period of increased speed immediately after each change in direction (Fig. 8). This burst of speed is not consistent with the more constant speeds observed during directional instability. It occurs because the trailing kinetochore loses all of its depolymerizing kMTs, and the remaining polymerizing kMTs grow sufficiently rapidly to remain fully inserted in the sleeves. The sleeves now slide on the MTs with their motion resisted only by the potential energy barrier associated with breaking interactions between tubulin subunits and their binding sites (see Eq. 7). When opposed only by this resistance, a large polar ejection force can push the chromosome at unnatural speeds. The reason for our prediction that kMTs polymerize at the in vitro rate of 40 subunits/s now becomes clear (see Polymerizing MTs above and Table 1). If the chromosome movement exceeds this rate, the tips of polymerizing kMTs at the trailing kinetochore get pulled into the sleeves, which then generate forces that break the chromosome (Eq. 7).

We were curious if our model could predict the force-speed relationship observed for chromosome movements during anaphase. By snagging chromosome arms with calibrated glass force-fibers, Nicklas (1983, 1988) measured the force developed during meiotic anaphase chromosome motion in insect spermatocytes. Nicklas observed that the speed of anaphase chromosome movement decreased as the imposed opposing force increased. To simulate this experiment, we modeled anaphase by considering only one kinetochore (no center spring connecting the sister kinetochores), and it was assumed that the relatively unopposed anaphase chromosome accumulates 30 depolymerizing MTs (Fig. 9). To mimic Nicklas' force-fiber, the chromosome movements are subjected to a linearly increasing force gradient of $120 \text{ pN}/\mu\text{m}$. The chromosome starts out at 52 nm/s ($3.1 \mu\text{m}/\text{min}$), which decreases to 20 nm/s ($1.2 \mu\text{m}/\text{min}$) when the opposing force reaches $\sim 150 \text{ pN}$. Thereafter, increased force has little effect on the speed of the chromosome until the chromosome loses all the depolymerizing

the spindle equator. The left kinetochore has five depolymerizing kMTs and hence becomes the leading kinetochore initially. (B and C) Total number of kMTs and the number of postcatastrophe kMTs at the left and right kinetochore, respectively. The number of postcatastrophe kMTs at the sister kinetochores decides which kinetochore leads. The trailing kinetochore loses kMTs that switch to shortening of the ejection forces are low and if the leading kinetochore has a larger number of such kMTs. (D) Force in the center spring as a result of the forces produced at both the kinetochores. The center spring is rarely compressed and shows a maximal extension of $\sim 1 \mu\text{m}$.

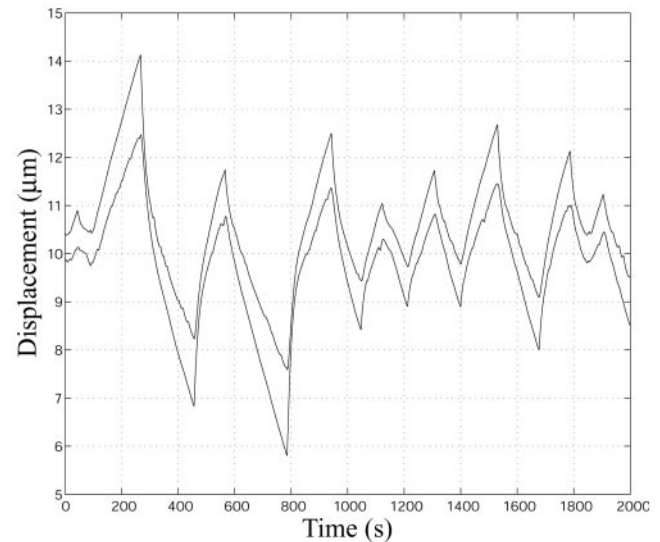
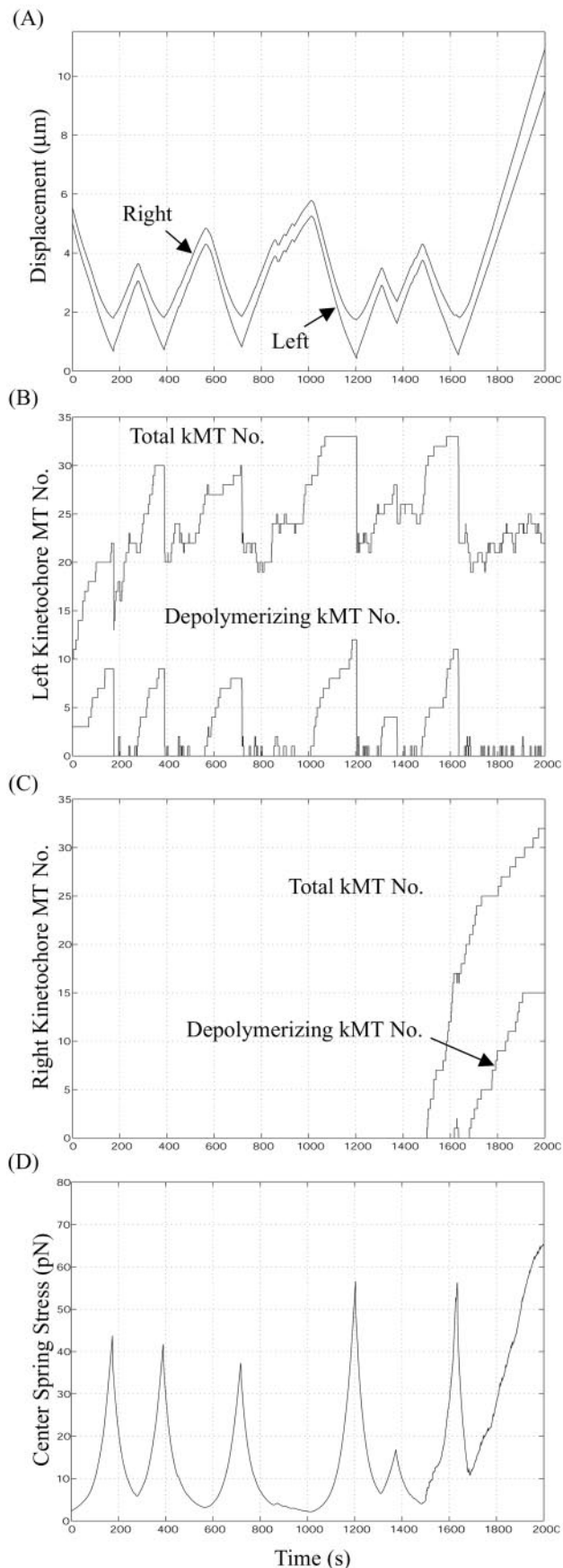


FIGURE 8 Effect of increased kMT polymerization rate on the simulated motion of a bioriented chromosome. kMTs polymerize at the in vivo rate (340 subunits/s) at which nonkinetochore MTs polymerize. The increased MT polymerization rate in the sleeve does not fundamentally change the oscillatory character of chromosome motion. The reduced resistance of the polymerizing kMTs on the trailing kinetochore however gives rise to higher speeds immediately after a direction reversal.

MTs at an opposing force of ~ 210 pN after ~ 80 s. Fig. 10 shows the normalized force-velocity curve that would be predicted from these data. For comparison we have also replotted the (normalized) force-velocity data that Nicklas estimated from his force-fiber experiments. The forces we observe are only approximately one-third to one-half of what Nicklas measured. This difference is not surprising as the experiments were performed using meiotic grasshopper spermatocytes, whereas the model uses parameters from mitotic mammalian (PtK1) cells. The important observation is that the model captures the general trend seen in the experiments.

DISCUSSION

We have developed a model that describes how the complex motions of mitotic chromosomes can arise from simple molecular kinetics and mechanical parameters. The model demonstrates that neither complex position sensing mechanisms, nor direct coordination of microtubule polymerization dynamics is required to explain directional instability of

FIGURE 7 (A) Simulated motion of a monooriented chromosome. The left kinetochore started off with three depolymerizing and seven polymerizing kMTs, whereas the right kinetochore was prevented from accumulating any MTs until 1500 s. (B and C) Number of total and depolymerizing kMTs at the left and right kinetochores, respectively. (D) Variations in the center-spring force as a function of time. The maximal extension of the spring in this case is ~ 0.5 μm .

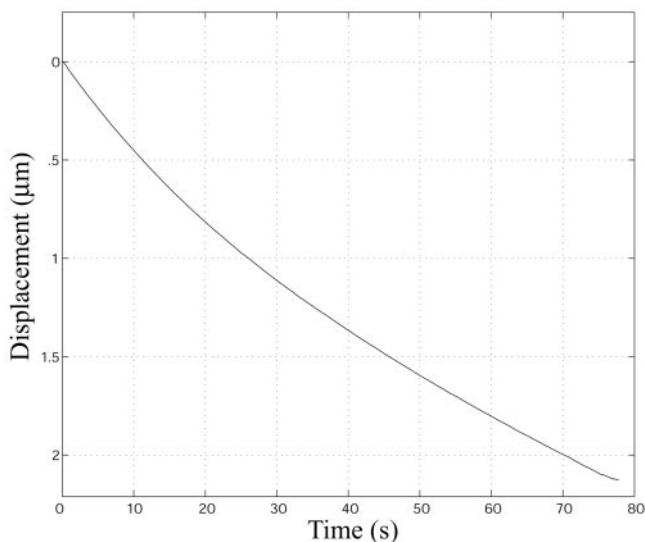


FIGURE 9 Simulation of Nicklas' monopolar chromosome snagging experiments (Nicklas, 1983). To simulate a microneedle, the ejection force increases linearly with the position, matching the typical stiffness of the microneedles (~ 120 pN/ μm). To simulate anaphase conditions, the kinetochores started out with 30 depolymerizing MTs.

chromosome movements. The model accurately predicts the speed and character of chromosome movements using parameters estimated from observed mitotic phenomena. We have tried to incorporate the most relevant available data about the structural and mechanical properties of chromosomes and the mitotic spindle. The direct and indirect data that have been used in this model are mostly obtained from experimental work on Potaroo Kidney cell lines. The details of the process will differ across species, but basic mechanisms and gross behaviors are likely to remain the same. For example, the mitotic spindle of budding yeast is considerably different from higher organisms, with chromosome segregation taking place inside the nuclear envelope and carried out by only a handful of MTs. Yet, the chromosomes seem also to undergo oscillatory motion (He et al., 2000). As discussed below, the model makes strong testable predictions to guide future experimentation.

Switching directions

Our model predicts that the load on a prometaphase-metaphase chromosome has little effect on the speed with which it moves, but strongly affects the probability of switching directions. This result is a direct consequence of the behavior of the force generating sleeves located at the kinetochores: the probability of kMT dissociation from a sleeve increases with load (Fig. 5, *A* and *B*), but the speed of movement remains constant over a wide range of loads. As a result, depolymerization-coupled movements of a chromosome maintain a constant speed even when working against an increasing load. Beyond a maximal load (which

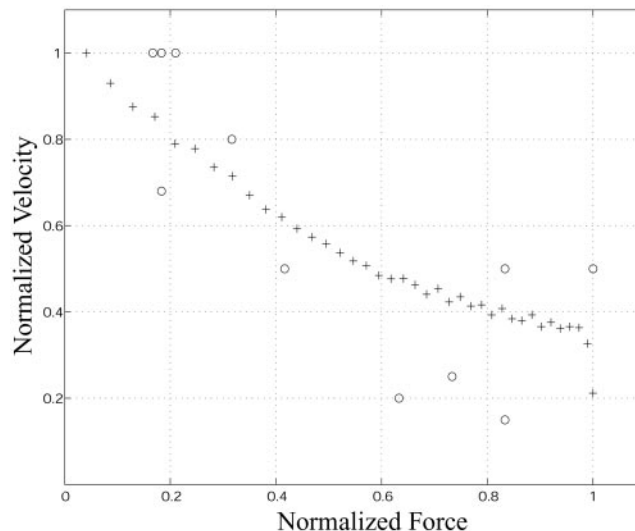


FIGURE 10 Graph of normalized force and velocity from Fig. 9. Dependence of velocity on force opposing the movement of an anaphase chromosome. The simulation results (+) are derived from the data shown in Fig. 7. For comparison, we have replotted the results observed by Nicklas (O) in meiotic insect cells (Nicklas, 1983). Both the axes are normalized to the maximal force and velocity. The normalized data implies that the model can predict the general behavior of the system under an elastic load. The actual values of forces obtained by Nicklas, however, are approximately twofold larger. This may be attributable to the differences across phyla and between mitosis and meiosis.

is proportional to the number of depolymerizing kMTs), one of the kinetochores loses all its depolymerizing MTs and no longer develops tension. This is in striking contrast to the behavior of ATP-dependent motor proteins, which are slowed by increased loads (Schnitzer et al., 2000; Meyhofer and Howard, 1995; Hunt et al., 1994; Svoboda and Block, 1994; Oiwa and Takahashi, 1988; Hill, 1938).

With this in mind we can explain how directional instability depends on stochastic interactions between kMTs and sleeves and the polar ejection force. Consider the sister kinetochores of a bioriented mitotic chromosome, each bound to a mix of polymerizing and depolymerizing kMTs. Initially both the kinetochores will follow the tips of depolymerizing kMTs, moving in opposite directions. The sister kinetochores will continue to separate until the tension across the kinetochores is great enough to cause some depolymerizing kMTs to detach. One of the kinetochores loses this tug-of-war when all of its depolymerizing kMTs detach, at which point it follows the now leading winner. As movement persists the leading kinetochore will accumulate depolymerizing kMTs as they undergo catastrophe. This accumulation of shortening kMTs increases the maximum force the kinetochore can develop. Consequently, the leading kinetochore will drag along the trailing kinetochore with sufficient force to cause it to lose any kMTs that switch from growth to rapid shortening. This can be seen in Fig. 6, *B* and *C*: a trailing kinetochore may acquire and lose many

kMTs. Thus, if there were no other forces, the leading kinetochore would tend to lead indefinitely. But as the chromosome moves closer to a pole, the ejection force opposing the leading kinetochore increases. Eventually this force becomes large enough that the additional force generated by even one or two shortening kMTs on the trailing kinetochore is sufficient to cause all shortening MTs on the leading kinetochore to detach. As a result the chromosome abruptly reverses the direction of motion, and the cycle begins anew (Fig. 6).

The importance of polar ejection forces is now clear: they bias the direction of chromosome motion toward the spindle equator (see also Khodjakov et al., 1999; Rieder and Salmon, 1994; Rieder et al., 1986). We assume that polar ejection forces arise from interactions between chromosomes and nonkinetochore MTs and are therefore proportional to the MT density and the size of the chromosome. In support of this, there is a strong correlation between MT density near a chromosome and the direction of chromosome movements (Cassimeris et al., 1994). Our model predicts that smaller chromosomes will exhibit longer excursions, bringing them closer to the spindle poles before they switch directions, but they should move at the same speed as larger chromosomes. The latter prediction is born-out by experimental observations (Nicklas, 1965). We have used a smooth ejection force distribution, which is constant over time. In all probability this is an oversimplification; the microtubule density undoubtedly exhibits spatial and temporal variations that could cause the direction of chromosome movements to switch less regularly than we predict, but gross features should be preserved.

It has been proposed descriptively that the prometaphase/metaphase movements of chromosomes could be explained if the two kinetochores on a bioriented chromosome independently switch between two movement states, "poleward" and "neutral," at 100 ± 10 -s intervals (Khodjakov et al., 1999). According to this hypothesis, the chromosome moves away from the proximal pole whenever both kinetochores are in the same state, otherwise the kinetochore in the "poleward" state leads. In the framework of our model, "poleward" and "neutral" states might correspond respectively to kinetochores containing shortening kMTs and those without. Also in agreement, our model does not require kinetochores to be "smart" (Khodjakov et al., 1999; Murray and Mitchison, 1994; Mitchison, 1989). But this is where the similarity ends: according to our model kinetochores do not switch between states independent of external parameters but instead due to stochastic microtubule dynamics and the bias that forces exert on mechanochemical transitions. A ramification of this is that sister kinetochores can simultaneously remain in the "poleward" state only briefly (Fig. 6).

Monopolar chromosomes

In Newt lung cells, during early prophase, one of the kinetochores of a chromosome associates laterally with a MT and glides rapidly along its surface toward the pole (Nicklas and Ward, 1994; Hayden et al., 1990). The speed of this motion (~ 300 nm/s or $18 \mu\text{m}/\text{min}$) is an order of magnitude faster than the typical speed of a bioriented chromosome (Skibbens et al., 1993). This is presumably due to ATP-dependent minus-end directed motor proteins located at or near the kinetochore of the chromosome. This rapid movement brings the monooriented chromosome into a region of high MT density, where the poleward facing kinetochore quickly forms multiple end-on attachments with the MTs. The monooriented chromosome then undergoes oscillatory movements toward and then away from the pole that are similar in velocity and character to the directional instability of a bioriented chromosome (Khodjakov and Rieder, 1996; Waters et al., 1996; Skibbens et al., 1993; Ault et al., 1991).

Fig. 7 A shows simulated oscillations of a monooriented chromosome. Initially the chromosome follows depolymerizing kMTs toward the pole, but as it approaches the pole the ejection force increases, and the kinetochore starts losing depolymerizing MTs. Soon there are only polymerizing MTs at the kinetochore, and the polar ejection force pushes the chromosome away from the pole. The polymerizing MTs can maintain attachments with the moving kinetochore, but MTs that switch to shortening are quickly lost. The probability of losing shortening MTs remains high as long as the chromosome is in the high ejection force region. However, as the chromosome moves away from the pole, the polar ejection force wanes and can be overpowered by kMTs that switch to shortening. We know of no quantitative descriptions of the spindle MT density during prometaphase, so we cannot deduce an explicit description for the polar ejection force distribution. We note that the model is relatively insensitive to the exact ejection force distribution; an inverse cube relation produces movements essentially identical to those shown in Fig. 7.

In early prometaphase, monooriented chromosomes exhibit oscillatory motions similar in character to those shown in Fig. 7. As mitosis progresses the oscillations sometimes become damped, and eventually even monooriented chromosomes move to the spindle equator (Khodjakov et al., 1997; Khodjakov and Rieder, 1996). Our model clearly predicts the latter behavior in the presence of an increasing polar ejection force, possibly due to elongation of spindle MTs accompanying spindle development from early prometaphase to metaphase. Damped oscillations are also a plausible outcome, but this depends heavily on the details of the spatial and temporal evolution of the ejection forces.

The role of motor proteins

The relatively constant speeds during directional instability are difficult to predict unless the speed of the underlying motors is substantially independent of the load. This brings out the challenge in producing directional instability solely from the ATP-dependent actions of conventional MT-based motor proteins. Increasing loads slow these motors, making it difficult to produce relatively constant speeds and abrupt changes in direction. If the load on the kinetochores changed, either due to loss of kMTs (thus increasing the load on remaining kMTs) or varying polar ejection forces, the speed of a chromosome would also change. Constant speed could be maintained if all of the motor proteins are always nearly unloaded. With this assumption, however, sudden changes in direction will require all motors on one kinetochore to be turned off as all motors on the sister kinetochore are turned on. It is difficult to envision a molecular mechanism for such exceptional physical coordination.

Nevertheless motor proteins are an integral part of the mitotic spindle and undoubtedly perform many important functions in mitosis (for review, see Maney et al., 2000). The motor proteins most relevant to directional instability are: chromokinesins located on the chromosome arms, motors located at the kinetochores such as CENP-E and dynein, and the motor-protein-like MT depolymerizing enzyme MCAK. Although our model does not directly posit a function for any of these molecules, we can deduce possible roles by considering how their activity and location could influence the model's behavior.

The minus-end-directed motor protein dynein has long been hypothesized to support poleward movements of chromosomes. Cytoplasmic dynein associates with the kinetochores in vertebrate as well as invertebrate mitotic systems (King et al., 2000; Pfarr et al., 1990; Vallee, 1990). In vertebrate cells, prometaphase kinetochores have more dynein associated with them than metaphase kinetochores (Escheverri et al., 1996; Pfarr et al., 1990). Similarly, in grasshopper spermatocytes, dynein transiently associates with the kinetochores, and this binding is regulated by MT attachment: most of the dynein dissociates from the kinetochores after they capture kMTs (King et al., 2000). This suggests that dynein facilitates early capture of spindle MTs and immediate rapid movements toward a pole, rather than directional instability, during which movements are slower by an order of magnitude (Nicklas and Ward, 1994; Skibbens et al., 1993; Hayden et al., 1990). In *Drosophila* embryo cells, cytoplasmic dynein is associated with the kinetochores throughout mitosis, and perturbations in its activity can alter the alignment of chromosomes at the spindle equator at metaphase (Sharp et al., 2000). Furthermore, depletion of dynein slows rapid chromosome motions that are variably observed throughout mitosis in *Drosophila* cells, although the slower movements are not attenuated

(Savoian et al., 2000; Sharp et al., 2000). This suggests additional roles for dynein during chromosome movements, at least in *Drosophila*. We propose that dynein acts as a supplemental force generator. Dynein motors located distal to the chromosome beyond the sleeves could increase the force driving chromosome movement without changing the fundamental character of directional instability. In this geometry chromosome movements could still be characterized by runs of relatively constant speed punctuated by sudden changes in direction, but the polar ejection force required to cause switching would be increased. This is because the force-generating behavior of the sleeves would still determine the force-velocity relationship. If a sleeve is unable to keep up with a shortening kMT, then the kMT will also depolymerize past the dynein motors. The load is then shifted to the other sleeves, which either rearrange to generate more force and continue to move at the same speed or lose their shortening MTs as well, resulting in a sudden reversal of the chromosome's direction. If the chromosome becomes substantially unloaded, dynein would aid kMTs to fully penetrate the sleeves, thus explaining the rapid dynein-dependent movements observed, for example, during late anaphase (Sharp et al., 2000).

The microtubule binding sites within a sleeve could in fact be motor-protein-like molecules. In this case they would serve as binding sites as described in our model, rather than the conventional ATP-dependent force generators. Such activity may explain the observation that motor-protein-coated microspheres will follow the ends of depolymerizing MTs, even in the absence of ATP (Lombillo et al., 1995b). The motor protein CENP-E might function in this way. CENP-E associates with the kinetochores during all the phases of mitosis and injection of antibodies directed against CENP-E results in unaligned chromosomes at metaphase in HeLa cells (Scharf et al., 1997) and loss of chromosome alignment in *Drosophila* cells at metaphase (Yucel et al., 2000). ATP-dependent motion of CENP-E is toward the plus end of MTs (Wood et al., 1997), thus this activity cannot be the source of the tension across kinetochores that predominates mitotic movements (Waters et al., 1996). However, in vitro depolymerization-coupled movements of chromosomes toward the minus ends of MTs can be disrupted by antibodies directed against CENP-E (Lombillo et al., 1995a), supporting a possible ATP-independent role in poleward force generation. CENP-E depletion affects the MT binding ability of kinetochores, causing misaligned and monopolar chromosomes along with spindle fragmentation (McEwen et al., 2001). These observations support a role for CENP-E in maintaining kMT contact with the kinetochores.

The association of motor-protein-like MCAK with the kinetochore has favorable implications for this model. MCAK localizes between the inner and outer plates of the kinetochores (Walczak et al., 1996; Wordeman and Mitchison, 1995) and can actively promote the loss of tubulin

subunits from the tips of microtubules (for review, see Hunter and Wordeman, 2000; Desai and Mitchison, 1995). We propose that MCAK prevents growing microtubules from producing forces at the kinetochores that could impede chromosome movements (Dogterom and Yurke, 1997). Given its location and activity, it is compelling to envision that MCAK trims the ends of microtubules that polymerize beyond the sleeves in the outer plate to keep them from impeding chromosome movements. This could be the molecular basis for our assertion that polymerizing MTs produce little force against the kinetochores.

Chromokinesin motors localize to chromosome arms and are an obvious candidate for the origin of polar ejection forces. Depletion of the chromokinesin *Xenopus*-Kid (Xkid) in *Xenopus* egg extracts has been shown to cause many phenotypes such as unaligned chromosomes at metaphase, chromosomes with their arms dragged toward the poles, uncondensed chromosomes, as well as abnormal spindle morphology such as shortened bipolar spindles and in other cases, monopolar spindles (Antonio et al., 2000; Funabiki and Murray, 2000). Most relevant to the model, chromokinesins appear to participate in the generation of polar ejection forces. In cultured human CPAC-1 cells injected with an antibody directed against the chromokinesin Kid, chromosome oscillations are suppressed, and chromosomes aggregate near the center of aberrant monopolar spindles (Levesque and Compton, 2001). These observations suggest that Kid generates polar ejection forces that push chromosomes away from spindle poles. Consistent with this, our model also predicts that suppressing polar ejection forces will cause chromosomes associated with one spindle pole to stop oscillating and move close to the pole. Interestingly, after the injection of Kid-specific antibodies, bioriented chromosomes still move full-speed toward the spindle equator, where they abruptly become nearly stationary (Levesque and Compton, 2001). This behavior appears to cast doubt on the role of polar ejection forces in directing chromosome movements to the spindle equator, and we were curious if our model could provide a plausible explanation. A critical clue is that during movement toward the spindle equator, the chromosomes are unusually oriented with their arms extending toward spindle poles. This suggests that without Kid to move chromosome arms toward the plus ends of MTs, the arms become ensnared or adhered to the mitotic spindle. In support of this, Funabiki et al. (2000) observed that many of the misaligned chromosomes in Xkid depleted *Xenopus* egg extracts appeared to be “held” in place, stretched with one end near the spindle equator, the other extending toward the pole. Our model predicts that if the resulting resistance comes to exceed the force that can be generated by one or two sleeves containing depolymerizing kMTs, a chromosome will become nearly stationary if the leading kinetochore loses its depolymerizing kMTs. This is because it is unlikely that either kinetochore will accumulate sufficient depolymerizing (i.e., force-

generating) kMTs to overcome the resistance and resume movement. Thus chromosome movement is suppressed.

But how then does a chromosome begin its run toward the equator in the first place (e.g., Fig. 7 A, starting at 1500 s)? This is feasible because when chromosomes are monooriented they are dragged near to the poles by their kinetochores, where even in the absence of Kid activity the arms are pushed away from the poles, possibly due to encounters with the dense array of MTs (Fig. 6 in Levesque and Compton, 2001). This indicates that although the character of the polar ejection forces is changed, near the poles they are not completely suppressed. Consequently there will be little resistance to movement of the leading kinetochore away from a pole immediately after a chromosome becomes bioriented; resistance will not build until the chromosome reorients to become strained in the opposite direction. The leading kinetochore may then have time to accumulate sufficient kMTs to develop the force necessary to drag the arms, at least to some extent, along the spindle MTs. This movement will cease when the leading kinetochore is overloaded nearer to the equator, possibly due to encounters with MTs emanating from the distal pole (Mastrorade et al., 1993), increased strain within the chromosome, or decreased residual ejection forces from the proximal pole. The relative importance of these effects is difficult to assess visually (Fig. 8 in Levesque and Compton, 2001), and may depend on the evolution of the spindle structure during mitosis. Suffice to say, we propose that at some point during the run to the equator a chromosome becomes stuck to the spindle, and thereafter there is little probability that the forces at the kinetochore will become large enough to unbind it.

Force, speed, and the number of kMTs

Our model accurately predicts the speed and form of chromosome movements, but is the magnitude of the forces appropriate? In grasshopper spermatocytes, Nicklas (1988) estimated the force on kinetochores during meiotic prometaphase from the observed strain on the chromosomes. With an estimated measurement error of $\pm 30\%$, he found the average force was typically in the range of 25 to 50 pN with extremes of ~ 100 pN. This shows striking consistency with our model, as is apparent from the strain across the kinetochores in Fig. 6 D. Can our model then be extended to explain the increased forces during anaphase? By stalling meiotic anaphase chromosomes with glass microneedles of known stiffness, Nicklas determined a maximal anaphase force on the order of 700 pN ($\pm 50\%$) (Nicklas, 1988, 1983). Assuming that polar ejection forces are reduced during anaphase, our model predicts that the kinetochores accumulate depolymerizing microtubules. So, the maximal force should approach $\sim 35 \times 15$ pN = 525 pN (15 pN is the maximal force that can be resisted by a depolymerizing MT in a sleeve, see Fig. 5). Thus, the predictions of our

model are consistent with anaphase force measurements, although this analysis neglects possible differences across species and meiosis versus mitosis. The model also captures the character of the relationship between force and velocity during anaphase (Fig. 10) within the error of the data.

We can now explain complex observations concerning the dependence of force at the kinetochore on the number of kMTs. When a kinetochore is partially damaged by irradiation by a focused laser to reduce the number of kMTs, the chromosome shifts to a new equilibrium position closer to the pole to which the unirradiated kinetochore is tethered (Hays and Salmon, 1990). This was interpreted as an indication that the poleward force depends on the number of kMTs, which leads to the prediction that chromosomes should move in the direction of the kinetochore with the most kMTs. But when moving chromosomes were chemically fixed and examined by electron microscopy, no such correlation was observed (McEwen et al., 1997). Both of these results can be explained by our model. Laser irradiation presumably destroys some fraction of the microtubule-binding sleeves. It thus reduces the number of potential force generating sites and decreases the average force generated at the kinetochore. But the force generated at a kinetochore depends on the number of postcatastrophe shortening kMTs more strongly than the total number of kMTs, and at any given moment there is little correlation between the number of kMTs and the direction of movement (Fig. 6, A–C). Although the model does predict that the number of MTs at the leading kinetochore will accumulate slowly, this will not be apparent until it has been leading for some time.

Eventually in the absence of an opposing force, both the total number of kMTs and the fraction depolymerizing will increase because loss of kMTs from the kinetochore will be suppressed. This can explain the increase in the number of kMTs (McEwen et al., 1997) as well as decreased kMT turnover (Zhai et al., 1995) that accompanies the onset of anaphase. Upon entry into anaphase opposing forces presumably diminish due to the separation of antagonistic sister kinetochores, and because depolymerization of non-kinetochore MTs decreases polar-ejection forces. If anaphase chromosome movement is only weakly opposed, kinetochore microtubules loss will be insignificant. The fivefold increase in the half-life of kinetochore microtubules upon entry into anaphase (Zhai et al., 1995) thus suggests that polar ejection forces are indeed significantly reduced.

APPENDIX

Rate constant for thermally induced movements, κ

This is the rate constant for discrete steps of a sleeve due to its random, thermal motion. It was originally derived assuming that a step required movement of the entire chromosome (Hill, 1985). This is inappropriate for our model, because sleeves move independently of the chromosome and

each other. A more suitable estimate is based on an approximate of the drag coefficient, ζ , for an individual sleeve. A sleeve must be larger than the 25-nm diameter of a microtubule and smaller than the distance between sleeves, 90 nm, so we approximate the sleeve as a sphere, 80 nm in diameter. This gives a Stokes drag coefficient, $\zeta = 6\pi\eta R = 7.5 \times 10^{-10} \text{ N s m}^{-1}$ ($= 7.5 \times 10^{-7} \text{ g s}^{-1}$), in which η ($= 1.0 \text{ mPa s}$) is viscosity, and R is radius. Following Hill (1985), this gives $\kappa = 15 \times 10^6 \text{ s}^{-1}$, which is approximately four orders of magnitude larger than that used by Hill. This is a rough estimate; it could easily be off by more than an order of magnitude due to friction within the kinetochore and the proximity of nearby surfaces (Happell and Brenner, 1965). However, the behavior of the model is only adversely affected if κ is much smaller, at which point the drag from sleeves containing fully inserted polymerizing MTs becomes large enough to overwhelm the force developed by sleeves with depolymerizing MTs. Increasing κ does not significantly change the model's behavior. Therefore we use a "worst-case scenario" that the drag coefficient on a sleeve is only one-fourth that of an entire chromosome, which following Hill (1985), gives $\kappa \cong 7200 \text{ s}^{-1}$. Running the model with this high rate would require an extremely short interval between iterations to assure that no events were missed; this causes simulations to run intolerably slow. To avoid this we model the kinetics of fully inserted growing microtubules using $\kappa = 7200 \text{ s}^{-1}$, but otherwise use Hill's original value in the simulation. We reiterate that using a lower value of κ for sleeves that are not fully penetrated has little effect on the model's behavior; it simply makes the simulation run faster.

Molecular roughness factor, r

Hill's model assumes a unit potential energy barrier, b , providing resistance to movement of the MT in a sleeve. The effect is accounted for by the factor, $r = e^{-b/kT} < 1$, which affects the rate that a MT shift between positions in the sleeve (see Eq. 3). The constraint, $r \leq 0.93$, used by Hill to prevent movements faster than observed physiological speeds, can now be relaxed; data gathered subsequently indicate forces that oppose chromosome movement are much greater than the 100-fN viscous drag assumed by Hill (Waters et al., 1996; Skibbens et al., 1993, 1995; Cassimeris et al., 1994; Rieder and Salmon, 1994; Nicklas, 1983, 1988). To estimate r , we assume that the 60-nm/s rate of poleward chromosome movement subsequent to depolymerization of nonkinetochore microtubules by nocodazole (Cassimeris and Salmon, 1991) is the speed that chromosomes move when essentially unloaded and calculate a corresponding value, $r = 0.96$.

Sleeves per kinetochore

McDonald et al. (1992) observed a slight preference for a spacing of ~ 90 nm between kMT neighbors, and we take this number to represent, at least functionally, the average distance between the centers microtubule binding sleeves. Taking the diameter of the kinetochores to be 600 nm (McEwen et al., 1993; McDonald et al., 1992; Rieder, 1982), we estimate the number binding sites for kMTs, $300^2/90^2 = 35$. We use a value of 35 based on electron microscopic data.

kMT catastrophe rate and on-rate, k_{cat} and k_{on}

Kinetochore microtubules must undergo catastrophe before they can be lost, thus the catastrophe rate is related the half-life, $t_{1/2}$, of kMTs, $k_{\text{cat}} = \ln(1/2)/t_{1/2}$. The half-life of kMTs is 4.7 min at 37°C (Zhai et al., 1995), giving $k_{\text{cat}} = 2.46 \times 10^{-3} \text{ s}^{-1}$. k_{on} to maintain the average number of kMTs at the observed value of 25 (Rusan et al., 2001; McEwen et al., 1997; McDonald et al., 1992) is given by, $k_{\text{on}} \times (\text{average empty sleeves}) = k_{\text{cat}} \times (\text{average kMTs})$, or, $k_{\text{on}} = k_{\text{cat}} \times 25/10$.

Central spring stiffness, K_{kinet}

Nicklas (1988) estimated the maximal stress on meiotic kinetochores in grasshoppers during prometaphase at ~ 100 pN. This estimate was made by examining chromosomal stretching, having earlier determined the compliance of the chromosome with a glass microneedle. The compliance is not relevant for our purposes because it reflects contributions across the length of two chromosomes in a meiotic bivalent, rather than the region between sister kinetochores. But it is reasonable, although not necessarily correct, to assume that the maximal stress is approximately the same during mitosis and across species. Taking the relaxed distance between PtK1 kinetochores at $\sim 0.5 \mu\text{m}$ and considering that the distance between sister kinetochores is often stretched more than twice the separation of kinetochores on unattached, relaxed chromosomes (Cimini et al., 2001; Waters et al., 1996; Skibbens et al., 1993), we estimate $K_{\text{kinet}} \sim 0.1$ pN/nm. The parameter determines how far apart sister kinetochores are stretched and how tightly the directional instability of sister kinetochores is coupled.

Sleeve spring stiffness, K_{sleeve}

To determine this value we examined kinetochore distortions in tomographic reconstruction electron micrographs of prometaphase/metaphase PtK1 cells, which were generously provided by Dr. J. R. McIntosh and the Boulder Laboratory for 3-D Fine Structure. The distortion of the outer plate rarely exceeds 100 nm between adjacent kMTs. The model predicts that in a kinetochore not at the extremes of its excursions, a typical maximal difference in strain between MTs will be around 7 pN (the difference between a polymerizing MT and a typically loaded depolymerizing MT). Thus, a good, albeit crude, estimate for the sleeve spring stiffness is, $K_{\text{sleeve}} = 7/100 = 0.07$ pN/nm. The model is relatively insensitive to the exact value of the parameter within a reasonable range. Each sleeve spring must have some compliance to exhibit physically realistic behavior, and we can eliminate extreme compliance that would result in greater kinetochore deformation than is actually observed. On this point, we note that certain types of mitotic failures can result in extreme kinetochore distortions exceeding one micron in the direction perpendicular to the distortions we considered in our estimate of K_{sleeve} (Cimini et al., 2001).

Matlab code used for these simulations can be found at: <http://www.umich.edu/~huntlab/projects.html>

We thank Dr. David D. Odde for providing a simulation of Hill's model that helped to inspire our thinking on this problem, and Dr. J. R. McIntosh, Dr. E. Meyhofer, and G. Brouhard for their comments on this work. We also thank Dr. D. Mastrorade and Dr. J. R. McIntosh, and the Boulder Laboratory for 3-D Fine Structure for sharing electron microscopy data on PtK1 spindle structures. This work was supported by the Burroughs Wellcome fund.

REFERENCES

Antonio, C., I. Ferby, H. Wilhelm, M. Jones, E. Karsenati, A. Nebreda, and I. Vernos. 2000. Xkid, a chromokinesin required for chromosome alignment on the metaphase plate. *Cell*. 102:425–435.

Ault, J. G., A. J. DeMarco, E. D. Salmon, and C. L. Rieder. 1991. Studies on the ejection properties of asters: astral microtubule turnover influences the oscillatory behavior and positioning of mono-oriented chromosomes. *J. Cell Sci.* 99:701–710.

Caplow, M., R. Ruhlen, and J. Shanks. 1994. The free energy for hydrolysis of a microtubule-bound nucleotide triphosphate is near zero: all of the free energy for hydrolysis is stored in the microtubule lattice. *J. Cell Biol.* 127:779–788.

Cassimeris, L., C. Rieder, and E. Salmon. 1994. Microtubule assembly and kinetochore directional instability in vertebrate monopolar spindles:

implications for the mechanism of chromosome congression. *J. Cell Sci.* 107:285–297.

Cassimeris, L., and E. Salmon. 1991. Kinetochore microtubules shorten by loss of subunits at the kinetochores of prometaphase chromosomes. *J. Cell Sci.* 98:151–158.

Cimini, D., B. Howell, P. Maddox, A. Khodjakov, F. Degrossi, and E. D. Salmon. 2001. Merotelic kinetochore orientation is a major mechanism of aneuploidy in mitotic mammalian tissue cells. *J. Cell Biol.* 153:517–527.

Desai, A., and T. Mitchison. 1995. A new role for motor proteins as couplers to depolymerizing microtubules. *J. Cell Biol.* 128:1–4.

Desai, A., and T. J. Mitchison. 1997. Microtubule polymerization dynamics. *Annu. Rev. Cell. Dev. Biol.* 13:83–117.

Dogterom, M., and B. Yurke. 1997. Measurement of the force-velocity relationship for growing microtubules. *Science*. 278:856–860.

Doorn, G. S. v., C. Tanase, B. Mudler, and M. Dogterom. 2000. On the stall force for growing microtubules. *Eur. Biophys. J.* 29:2–6.

Escheverri, C. J., B. M. Paschal, K. T. Vaughan, and R. B. Vallee. 1996. Molecular characterization of the 50-kD subunit of dynactin reveals the function for the complex in chromosome alignment and spindle organization during mitosis. *J. Cell Biol.* 132:617–633.

Funabiki, H., and A. Murray. 2000. The *Xenopus* chromokinesin Xkid is essential for metaphase chromosome alignment and must be degraded to allow anaphase chromosome movement. *Cell*. 102:411–424.

Gorbsky, G., P. Sammak, and G. Borisy. 1987. Chromosomes move poleward in anaphase along stationary microtubules that coordinately disassemble from their kinetochore ends. *J. Cell Biol.* 104:9–18.

Happell, J., and H. Brenner. 1965. Low Reynold's Number Hydrodynamics. Prentice-Hall, Englewood Cliffs, NJ.

Hayden, J., S. Bowser, and C. Rieder. 1990. Kinetochores capture astral microtubules during chromosome attachment to the mitotic spindle: direct visualization in live newt lung cells. *J. Cell Biol.* 111:1039–1045.

Hays, T. S., and E. D. Salmon. 1990. Poleward force at the kinetochore in metaphase depends on the number of kinetochore microtubules. *J. Cell Biol.* 110:391–404.

He, X., S. Asthana, and P. Sorger. 2000. Transient sister chromatid separation and elastic deformation of chromosomes during mitosis in budding yeast. *Cell*. 101:763–775.

Hill, A. 1938. The heat of shortening and the dynamic constants in muscle. *Proc. R. Soc. Lond.* 126:136–195.

Hill, T. 1985. Theoretical problems related to the attachment of microtubules to kinetochores. *Proc. Natl. Acad. Sci. U.S.A.* 82:4404–4408.

Hill, T. 1987. Linear Aggregation Theory in Cell Biology. Springer-Verlag, New York.

Hunt, A., and J. McIntosh. 1998. The dynamic behavior of individual microtubules associated with chromosomes in vitro. *Mol. Biol. Cell*. 9:2857–2871.

Hunt, A. J., F. Gittes, and J. Howard. 1994. The force exerted by a single kinesin molecule against a viscous load. *Biophys. J.* 67:766–781.

Hunter, A. W., and L. Wordeman. 2000. How motor proteins influence microtubule polymerization dynamics. *J. Cell Sci.* 113:4379–4389.

Khodjakov, A., R. Cole, B. McEwen, K. Buttle, and C. Rieder. 1997. Chromosome fragments possessing only one kinetochore can congress to the spindle equator. *J. Cell Biol.* 136:229–240.

Khodjakov, A., I. S. Gabashvili, and C. L. Rieder. 1999. "Dumb" versus "smart" kinetochore models for chromosome congression during mitosis in vertebrate somatic cells. *Cell Motil. Cytoskeleton*. 43:179–185.

Khodjakov, A., and C. L. Rieder. 1996. Kinetochores moving away from their associated pole do not exert a significant pushing force on the chromosome. *J. Cell Biol.* 135:315–327.

King, J., T. S. Hays, and R. B. Nicklas. 2000. Dynein is a transient kinetochore component whose binding is regulated by microtubule attachment, not tension. *J. Cell Biol.* 151:739–748.

Kolomeisky, A., and M. Fisher. 2001. Force-velocity relation for growing microtubules. *Biophys. J.* 80:149–154.

- Levesque, A., and D. Compton. 2001. The chromokinesin kid is necessary for chromosome arm orientation and oscillation, but not congression, on mitotic spindles. *J. Cell Biol.* 154:1135–1146.
- Lombillo, V., C. Nislow, T. J. Yen, V. Gelfand, and J. McIntosh. 1995a. Antibodies to the kinesin motor domain and CENP-E inhibit microtubule depolymerization-dependent motion of chromosomes in vitro. *J. Cell Biol.* 127:108–115.
- Lombillo, V., R. Stewart, and J. McIntosh. 1995b. Minus-end-directed motion of kinesin-coated microspheres driven by microtubule depolymerization. *Nature.* 373:161–164.
- Maney, T., L. Ginkel, A. W. Hunter, and L. Wordeman. 2000. The kinetochore of higher eucaryotes: a molecular view. *Int. Rev. Cytol.* 194:67–131.
- Mastronarde, D., K. McDonald, R. Ding, and J. McIntosh. 1993. Interpolar spindle microtubules in PTK cells. *J. Cell Biol.* 123:1475–1489.
- McDonald, K., E. O'Toole, D. Mastronarde, and J. McIntosh. 1992. Kinetochore microtubules in PTK cells. *J. Cell Biol.* 118:369–383.
- McEwen, B., J. Arena, J. Frank, and C. Rieder. 1993. Structure of the colcemid-treated PTK1 kinetochore outer plate as determined by high voltage electron microscopic tomography. *J. Cell Biol.* 120:301–312.
- McEwen, B., G. Chan, B. Zubrowski, M. Savoian, M. Sauer, and T. J. Yen. 2001. CENP-E is essential for reliable bioriented spindle attachment, but chromosome alignment can be achieved via redundant mechanisms in mammalian cells. *Mol. Biol. Cell.* 12:2776–2789.
- McEwen, B., A. Heagle, G. Cassels, K. Buttle, and C. L. Rieder. 1997. Kinetochore fiber maturation in PtK1 cells and its implications for the mechanisms of chromosome congression and anaphase onset. *J. Cell Biol.* 137:1567–1580.
- Meyhofer, E., and J. Howard. 1995. The force generated by a single kinesin molecule against an elastic load. *Proc. Natl. Acad. Sci. U.S.A.* 92:574–578.
- Mickey, B., and J. Howard. 1995. Rigidity of microtubules is increased by stabilizing agents. *J. Cell Biol.* 130:909–917.
- Mitchison, T. 1989. Chromosome alignment in at mitotic metaphase: balance of forces or smart kinetochores? *Cell Movement.* 2:421–430.
- Mitchison, T., L. Evans, E. Schulze, and M. Kirschner. 1986. Sites of microtubule assembly and disassembly in the mitotic spindle. *Cell.* 45:515–527.
- Mitchison, T., and M. Kirschner. 1984. Dynamic instability of microtubule growth. *Nature.* 312:237–242.
- Mitchison, T., and E. Salmon. 1992. Poleward kinetochore fiber movement occurs during both metaphase and anaphase-A in newt lung cell mitosis. *J. Cell Biol.* 119:569–582.
- Mogilner, A., and G. Oster. 1999. The polymerization ratchet model explains the force-velocity relation for growing microtubule. *Eur. Biophys. J.* 28:235–242.
- Murray, A., and T. Mitchison. 1994. Kinetochores pass the IQ test. *Curr. Biol.* 4:38–41.
- Nicklas, R. 1965. Chromosome velocity during mitosis as a function of chromosome size and position. *J. Cell Biol.* 25:119–135.
- Nicklas, R. 1983. Measurements of the force produced by the mitotic spindle in anaphase. *J. Cell Biol.* 97:542–548.
- Nicklas, R. 1988. The forces that move chromosomes in mitosis. *Annu. Rev. Biophys. Biophys. Chem.* 17:431–449.
- Nicklas, R. B., and S. C. Ward. 1994. Elements of error correction in mitosis: microtubule capture, release, and tension. *J. Cell Biol.* 126:1241–1253.
- Oiwa, K., and K. Takahashi. 1988. The force-velocity relationship for microtubule sliding in demembrated sperm flagella of the sea urchin. *Cell Struct. Funct.* 13:193–205.
- Pfarr, C., M. Coue, P. Grissom, T. Hays, M. Porter, and J. McIntosh. 1990. Cytoplasmic dynein is localized to kinetochores during mitosis. *Nature.* 345:263–265.
- Rieder, C., S. Alexander, and G. Rupp. 1990. Kinetochores are transported poleward along a single astral microtubule during chromosome attachment to the spindle in newt lung cells. *J. Cell Biol.* 110:81–95.
- Rieder, C., E. Davidson, L. Jenesen, L. Cassimeris, and E. Salmon. 1986. Oscillatory movements of mono-oriented chromosomes and their position relative to the spindle pole result from the ejection properties of the asters and half-spindle. *J. Cell Biol.* 103:581–591.
- Rieder, C., and E. Salmon. 1994. Motile kinetochores and polar ejection forces dictate chromosome position on the vertebrate mitotic spindle. *J. Cell Biol.* 124:223–233.
- Rieder, C., and E. Salmon. 1998. The vertebrate cell kinetochore and its roles during mitosis. *Trends Cell Biol.* 8:310–318.
- Rieder, C. L. 1982. The formation, structure, and composition of the mammalian kinetochore and kinetochore fiber. *Int. Rev. Cytol.* 79:1–58.
- Rusan, N., C. Fagerstrom, A. Yvon, and P. Wadsworth. 2001. Cell cycle dependent changes in microtubule dynamics in living cells expressing green fluorescent protein-alpha tubulin. *Mol. Biol. Cell.* 12:971–980.
- Savoian, M., M. Goldberg, and C. L. Rieder. 2000. The rate of poleward chromosome motion is attenuated in *Drosophila* zw10 and rod mutants. *Nat. Cell Biol.* 2:948–952.
- Scharr, B., G. Chan, P. Maddox, E. D. Salmon, and T. J. Yen. 1997. CENP-E function at kinetochore is essential for chromosome alignment. *J. Cell Biol.* 139:1373–1382.
- Schnitzer, M., K. Visscher, and S. Block. 2000. Force produced by single kinesin motors. *Nat. Cell Biol.* 2:718–723.
- Sharp, D., G. Rogers, and J. Scholey. 2000. Cytoplasmic dynein is required for poleward chromosome movement during mitosis in *Drosophila* embryos. *Nat. Cell Biol.* 2:922–930.
- Skibbens, R., C. Rieder, and E. Salmon. 1995. Kinetochore motility after severing between sister centromeres using laser microsurgery: evidence that kinetochore directional instability and position is regulated by tension. *J. Cell Sci.* 108:2537–2548.
- Skibbens, R., V. Skeen, and E. Salmon. 1993. Directional instability of kinetochore motility during chromosome congression and segregation in mitotic newt lung cells: a push-pull mechanism. *J. Cell Biol.* 122:859–875.
- Svoboda, K., and S. Block. 1994. Force and velocity measured for single kinesin molecules. *Cell.* 77:773–784.
- Vallee, R. 1990. Dynein and the kinetochore. *Nature.* 345:206–207.
- Walczak, C., T. Mitchison, and A. Desai. 1996. XKCM1: A *Xenopus* kinesin-related protein that regulates microtubule dynamics during mitotic spindle assembly. *Cell.* 84:37–47.
- Walker, R., E. O'Brien, N. Pryer, W. Voter, H. Erickson, and E. Salmon. 1988. Dynamic instability of individual microtubules analyzed by video light microscopy: rate constants and transition frequencies. *J. Cell Biol.* 107:1437–1448.
- Waters, J., R. Skibbens, and E. Salmon. 1996. Oscillating mitotic newt lung cell kinetochores are, on average, under tension and rarely push. *J. Cell Sci.* 109:2823–2831.
- Wise, D., L. Cassimeris, C. L. Rieder, P. Wadsworth, and E. D. Salmon. 1991. Chromosome fiber dynamics and congression oscillations in metaphase PtK2 cells at 23 degrees C. *Cell Motil. Cytoskeleton.* 18:131–142.
- Wood, K., R. Sakowicz, L. Goldstein, and D. Cleveland. 1997. CENP-E is a plus end-directed kinetochore motor required for metaphase chromosome alignment. *Cell.* 91:357–366.
- Wordeman, L., and T. J. Mitchison. 1995. Identification and partial characterization of mitotic centrosome-associated kinesin, a kinesin-related protein that associates with centromeres during mitosis. *J. Cell Biol.* 128:95–105.
- Yucel, J., J. Marszalek, J. McIntosh, L. Goldstein, D. Cleveland, and A. Philip. 2000. CENP-meta, an essential kinetochore kinesin required for the maintenance of metaphase chromosome alignment in *Drosophila*. *J. Cell Biol.* 150:1–11.
- Zhai, Y., P. J. Kronebusch, and G. G. Borisy. 1995. Kinetochore microtubule dynamics and the metaphase-anaphase transition. *J. Cell Biol.* 131:721–734.